Title

Association Between Thoracic Spinal Cord Gray Matter Atrophy and Disability in Multiple Sclerosis

Journal

JAMA Neurology, 72(8)

ISSN

2168-6149

Authors

Schlaeger, Regina

Papinutto, Nico

Zhu, Alyssa H

et al.

Publication Date

2015-08-01

DOI

10.1001/jamaneurol.2015.0993

Peer reviewed

HHS Public Access

Author manuscript

JAMA Neurol. Author manuscript; available in PMC 2018 June 15.

Published in final edited form as:

JAMA Neurol. 2015 August ; 72(8): 897–904. doi:10.1001/jamaneurol.2015.0993.

The association between thoracic spinal cord gray matter atrophy and disability in Multiple Sclerosis

Regina Schlaeger, MD[1,2], **Nico D. Papinutto, PhD**[1], **Alyssa H. Zhu, MSc**[1], **Iryna V. Lobach, PhD**[1,3], **Carolyn J. Bevan, MD, MS**[1], **Monica Bucci, MD**[1], **Antonella Castellano, MD**[1], **Jeffrey M. Gelfand, MD, MAS**[1], **Jennifer S. Graves, MD, PhD, MAS**[1], **Ari J. Green, MD, MCR**[1,4], **Kesshi M. Jordan, BS**[1,6], **Anisha Keshavan, BS**[1,6], **Valentina Panara, MD**[1], **William A. Stern, RT (MR)**[1], **H.-Christian von Büdingen, MD**[1], **Emmanuelle Waubant, MD, PhD**[1], **Douglas S. Goodin, MD**[1], **Bruce A. C. Cree, MD, PhD, MAS**[1], **Stephen L. Hauser, MD**[1], and **Roland G. Henry, PhD**[1,5,6]

[1]Department of Neurology, University of California San Francisco, USA [2]Department of Neurology, University Hospital Basel, University of Basel, Switzerland [3]Departments of Epidemiology and Biostatistics, University of California San Francisco, USA [4]Department of Ophthalmology, University of California San Francisco, USA [5]Department of Radiology and Biomedical Imaging, University of California San Francisco, USA [6]Bioengineering Graduate Group, University of California San Francisco & Berkeley, USA

Abstract

Importance—In multiple sclerosis (MS), upper cervical cord gray matter (GM) atrophy correlates more strongly with disability than does brain or cord white matter (WM) atrophy. The corresponding relationships in the thoracic cord are unknown owing to technical difficulties in assessing GM and WM compartments by conventional magnetic resonance imaging techniques.

Objectives—To investigate the associations between MS disability and disease type with lower thoracic cord GM and WM areas using phase-sensitive inversion recovery magnetic resonance imaging at 3T, as well as to compare these relationships with those obtained at upper cervical levels.

Design, Setting, and Participants—Between July 2013 and March 2014, a total of 142 patients with MS (aged 25-75 years; 86 women) and 20 healthy control individuals were included in this cross-sectional observational study conducted at an academic university hospital.

Main Outcomes and Measures—Total cord areas (TCAs), GM areas, and WM areas at the disc levels C2/C3, C3/C4, T8/9, and T9/10. Area differences between groups were assessed, with age and sex as covariates.

Results—Patients with relapsing MS (RMS) had smaller thoracic cord GM areas than did age- and sex-matched control individuals (mean differences [coefficient of variation (COV)]: 0.98 mm2

Corresponding Author: Regina Schlaeger, MD; 675 Nelson Rising Lane, BOX 3206, San Francisco, CA 94158, USA, Phone: +1 415 425 8266; regina.schlaeger@ucsf.edu.

None of these potential conflicts of interest are relevant to this study.

[9.2%]; P = .003 at T8/T9 and 0.93 mm2 [8.0%]; P = .01 at T9/T10); however, there were no significant differences in either the WM area or TCA. Patients with progressive MS showed smaller GM areas (mean differences [COV]: 1.02 mm2 [10.6%]; P < .001 at T8/T9 and 1.37 mm2 [13.2%]; P < .001 at T9/T10) and TCAs (mean differences [COV]: 3.66 mm2 [9.0%]; P < .001 at T8/T9 and 3.04 mm2 [7.2%]; P = .004 at T9/T10) compared with patients with RMS. All measurements (GM, WM, and TCA) were inversely correlated with Expanded Disability Status Scale score. Thoracic cord GM areas were correlated with lower limb function. In multivariable models (which also included cord WM areas and T2 lesion number, brain WM volumes, brain T1 and fluid-attenuated inversion recovery lesion loads, age, sex, and disease duration), cervical cord GM areas had the strongest correlation with Expanded Disability Status Scale score followed by thoracic cord GM area and brain GM volume.

Conclusions and Relevance—Thoracic cord GM atrophy can be detected in vivo in the absence of WM atrophy in RMS. This atrophy is more pronounced in progressive MS than RMS and correlates with disability and lower limb function. Our results indicate that remarkable cord GM atrophy is present at multiple cervical and lower thoracic levels and, therefore, may reflect widespread cord GM degeneration.

Introduction

Spinal cord (SC) atrophy in multiple sclerosis (MS) is a common and clinically important aspect of the disease.[1,2] and may be one of the principal substrates of MS progression.[3] A reduction in the cross-sectional upper cervical cord area, as detected *in vivo* by MRI, has been documented throughout the disease course, both in cross-sectional and longitudinal analyses.[4–12] This reduction is often considered to reflect axonal loss,[13–15] although it is likely that other processes such as loss of SC neurons[16] and myelin[17] also contribute.

Until recently, the relative contributions of white matter (WM) and gray matter (GM) loss to the overall reduction of SC volume in MS patients could only be assessed in post-mortem studies, which provide conflicting results.[18,14] Fixation artifacts that cause unpredictable swelling, shrinkage or tissue deformation complicate post-mortem studies[19] and can affect GM and WM differently.[20] The *in vivo* assessment of SC GM and WM compartments was limited by insufficient contrast between GM and WM on conventional imaging and by artifacts related to physiological motion of the cord and adjacent tissues.[21,22]

Phase sensitive inversion recovery (PSIR) imaging[23,24] has been used in MS to characterize lesions and to estimate total cord areas (TCA).[25,26] Our group recently developed a sensitive method to detect SC GM atrophy based on 2D-PSIR image acquisitions that enable reliable assessment of TCAs, GM and WM structures in clinically feasible scanning times (<2min/level).[27] Using this method, we demonstrated that the upper cervical SC GM can be reduced in RMS in the absence of WM atrophy, and that GM atrophy is substantially more pronounced in PMS compared to RMS.[28] In addition, the cervical SC GM area was inversely correlated with disability.

The objective of this study was to assess the associations between GM/WM compartments of the lower thoracic cord with measures of clinical disability and disease type in a large,

single-center cohort of MS patients. A secondary goal was to compare these relationships with those obtained at the upper cervical levels.

Design and methods

Research participants

This study included 142 MS[29] patients seen at the UCSF Multiple Sclerosis Center between 7/2013 and 3/2014 as part of an observational study. Inclusion and exclusion criteria are listed in the eMethods (Supplement). We also studied 20 healthy control subjects, who were age- and sex-matched with the RMS group. The Committee on Human Research at UCSF approved the study protocol. Written informed consent was obtained from all participants.

Clinical assessments

All patients were assessed by the Neurostatus/Expanded Disability Status Scale (EDSS), Timed 25-Foot Walk Test (T25FW) and 9-Hole Peg Test (9-HPT).[30–32] Hip flexion strength was evaluated and graded according to the Medical Research Council (MRC) scale. Results from each side were added to a score from 0-10 (with 10 indicating full strength bilaterally).

Image acquisition

All participants were scanned at the same 3T MR-scanner, patients within two weeks of their clinical evaluation. Axial 2D-PSIR images were acquired perpendicular to the SC at the C2/C3, C3/C4, T8/T9 and T9/T10 intervertebral disc levels (Fig. 1). We chose the disc level T9/T10 (corresponding to the segmental level of L1/L2), both because the GM at this cord level is involved in proximal leg function, and because it is sufficiently removed from the lumbar enlargement (where the anatomic inter-subject variability is thought to be greater) and from rostral thoracic segments (where imaging artifacts can be substantial).

In addition, the patients underwent standard high-resolution T1-weighted and 3D-FLAIR images of the brain; T2-weighted sagittal and axial images of the cervical cord and sagittal images of the thoracic cord. For detailed acquisition parameters s. eMethods.

Image analysis

TCAs and SC GM areas at all four levels were measured on the phase-sensitive reconstructed images using the software JIM6 (Xinapse systems, www.xinapse.com) (Fig. 1). Reliability assessments have previously been published for this segmentation methodology.[27] Based on these results, GM and TCA assessments were made by a single reader (RS), who was masked to the clinical data. TCA measurements were performed in a semi-automated fashion.[33] SC GM areas were manually segmented as described previously.[28]

Analyses of brain MPRAGE, FLAIR and SC T2-images are described in the eMethods.

Statistical analysis

Correlations between PSIR-derived measures and clinical characteristics (EDSS, T25FW, 9-HPT, hip flexion strength) were assessed using Spearman rank correlation due to the non-

normal distribution of clinical characteristics. The Bonferroni method was performed to correct for multiple comparisons across two independent cord areas at four levels for four clinical metrics (correction factor 32). Similarly, the comparison of PSIR-derived measures between cord levels was performed using Spearman rank correlation due to the non-normal distribution of WM areas at C3/C4 and T9/T10. Linear regression analyses were used to estimate differences in PSIR-derived measures at each level between controls, RMS and PMS patients adjusting first for age and sex and secondly for sex and disease duration.

The relative contribution of demographics, clinical characteristics, and PSIR-derived measures to the observed EDSS variability were investigated using analyses of relative importance of regressors in a linear model (RELAIMPO package in R).[34,35] Specifically, the relative contribution of cervical and thoracic SC GM areas to EDSS was quantified along with the following variables: cervical and thoracic SC WM areas, normalized brain GM and WM volumes, brain T1-lesion and FLAIR-lesion volumes, SC lesion number, age, sex, disease duration. The variables with the largest contribution to EDSS were further examined for an association with the probability of a progressive disease course (adjusted for age) based on probability maps.

Moreover, receiver operating characteristic (ROC) curves were compiled (eMethods). Partial regression analysis was performed to assess the added value of thoracic SC GM areas in correlating with EDSS while adjusting for other variables (including cervical SC GM areas) (eMethods). The levels T9/T10 and C2/C3 were selected for this analysis because they had previously been shown to have the highest measurement reliability in the thoracic and cervical cord,[27] and additionally demonstrated consistently good image quality in the present cohort.

Results

Demographic and clinical characteristics are summarized in e-Table 1. Of the 142 MS patients, 99 had a relapsing and 43 had a progressive disease course.[36] The control group showed similar distributions of age and sex compared to the RMS patients (e-Table 1). GM segmentation was impossible due to image distortion by either motion or lesion artifacts in 9%, 9%, 15% and 12% of the images at the levels C2/C3, C3/C4, T8/T9, T9/T10 respectively.

At all four levels, there was an inverse correlation of the EDSS with the SC GM area (C2/C3: ρ=-0.64, C3/C4:-0.63, T8/T9:-0.47, T9/T10:-0.48, all $p<0.001$), with the SC WM area (C2/C3: ρ=-0.36, C3/C4:-0.30, T8/T9:-0.33, T9/T10:-0.37, all $p\leq0.001$), and with the TCA (C2/C3: ρ=-0.48, C3/C4:-0.45, T8/T9:-0.41, T9/T10:-0.40, all $p<0.001$). Moreover, the T25FW showed significant inverse correlations with the GM areas, WM areas and TCAs at all levels (all $p<0.001$). These associations all remained significant after Bonferroni correction (e-Table 2).

The 9-HPT showed significant moderate negative associations only with the TCA and SC GM area at the cervical levels, but not at the thoracic levels after correction for multiple comparisons (e-Table 2).

Hip flexion strength was moderately correlated with thoracic SC GM areas (ρ=0.52, p<0.001) and WM areas (ρ=0.40, p<0.001) at T9/10 and also at T8/T9 (ρ=0.42, p<0.001; ρ=0.39, p<0.001, respectively) and showed significant correlations with thoracic SC GM areas, independently from EDSS. On the other hand, hip flexion strength did not show a significant association with cervical SC GM areas when accounting for EDSS.

TCAs, cord GM and WM areas showed significant moderate to strong correlations with the corresponding measures at all other levels, with particularly strong associations between corresponding measures at adjacent levels (e-Table 3).

When adjusted either for age and sex (Table 1) or for disease duration and sex (e-Table 4), the mean SC GM areas and TCAs at all levels were significantly smaller in PMS patients compared to RMS patients, while the SC WM areas were only significantly different at the two cervical levels.

RMS patients had significantly smaller mean GM areas at C2/C3, T8/T9 and T9/T10 compared to controls. GM areas at C3/C4 also followed this trend, but did not reach statistical significance. No significant differences in SC WM areas and TCAs were found between these groups at any level.

The analyses of relative contribution of age, sex, disease duration, the PSIR-derived cord measures along with brain WM and GM volumes, T1- and FLAIR-lesion loads and SC lesion number demonstrated statistically significant contributions of all variables to EDSS variance. Fig. 2 shows the relative contributions of GM and WM areas at C2/C3 and T9/T10 along with all other variables, normalized to sum 100% of explained variance in EDSS. The GM area at C2/C3 had the highest relative importance in predicting EDSS of all variables (0.41; 95% CI 0.21-0.52), followed next by the GM area at T9/T10 (0.20; 95% CI 0.06–0.33) and the normalized brain GM volume (0.12; 95% CI 0.03-0.24). This order of relative importance remained the same among variables regardless of the chosen combination of cervical and thoracic levels.

The results of the corresponding analyses with the 9-HPT and the T25FW as outcomes are shown in e-Figure 1A–B.

The C2/C3 and T9/T10 SC GM areas each contributed significant added value to accounting for EDSS variance, both in bivariable and multivariable regression models. Analysis of the importance of the SC GM measures relative to all other variables, i.e. when the SC measures entered the multivariable model last, reached similar conclusions (e-Table 5).

Probability maps demonstrated a significant association between cervical (Fig. 3A, B) and thoracic GM area measures (Fig. 3C, D), respectively, and the probability of a progressive (vs. relapsing) disease course adjusted for age.

E-Fig. 2 displays ROC curves for the prediction of a progressive disease course by logistic models with the SC GM areas at each level as single predictors (A), and cervical and thoracic GM areas as combined predictors (B). The areas under the ROC curve (AUC) were

0.84, 0.83, 0.72 and 0.78 for the models based on SC GM area at the levels C2/C3, C3/C4, T8/T9 and T9/T10, respectively (e-Table 6).

Fig. 4 displays the ROC curves for the models based on (a) brain GM volume, (b) the combination of brain GM volume and SC GM area at T9/T10, and (c) the combination of brain GM volume with SC GM areas at C2/C3 and T9/T10 as predictors of a progressive versus relapsing disease course. The AUCs were 0.68, 0.79 and 0.87, respectively. The AUC of model c was significantly higher than the AUC for model a (p=0.003). Model c predicted a progressive disease course with a sensitivity and specificity of 0.81 and 0.80, respectively.

Discussion

Our results provide *in vivo* evidence of a significant association between the lower *thoracic* cord GM area and both MS disability and disease type.

In the lower *thoracic* cord, RMS patients demonstrated selective GM atrophy. PMS patients showed more substantial GM and TCA reductions than did RMS patients. A model based on cervical and thoracic cord GM matter area together with brain GM predicted a progressive disease course with a sensitivity of 0.81 and a specificity of 0.80. This model was superior to one based on brain GM alone. These findings extend and confirm the results of our recent report that quantitated upper *cervical* GM atrophy in a larger cohort including an increased number of progressive patients.

Lower thoracic cord GM areas were inversely correlated with EDSS. Cervical and thoracic GM areas consistently had the greatest relative contribution to EDSS in multivariable regression analyses, followed by brain GM volume. Interestingly, thoracic cord GM contributed *independently* to EDSS, even when the cervical GM area was accounted for. Both measures are reflective of a global process of GM degeneration in MS, but at the same time also convey regional information concerning atrophy. While there is a global SC GM atrophy that is present throughout the cord cervical and thoracic levels, there may be individual variations within the thoracic cord superimposed that have direct functional consequences, which provide additional explanatory power for EDSS. We observed a moderate, but significant association between the thoracic GM area at the disc level T9/T10 and the strength of muscles (i.e. iliopsoas) innervated by the corresponding segmental level (L1/L2). In line with this observation, 9-HPT was only correlated with SC GM areas at cervical levels, not at thoracic levels. These observations highlight potential clinical correlates of cord GM atrophy at a regional level.

Only a few MR studies to date have investigated the thoracic cord in MS, and none have segregated the GM and WM compartments and assessed their relation to disability and disease type. Liu *et al.*[37] reported a reduction of cervical TCAs in a relatively small, heterogeneous MS group, but only a trend towards TCA reductions in the thoracic cord was found. The higher degree of total cord atrophy in the cervical compared to the thoracic region is in line with our findings.

Consistent with our findings, Klein *et al,.*[38] found significant cord volume reductions in PMS compared to RMS. In contrast to Liu's and our observations, they described a trend

towards increased cervical and thoracic cord volumes in RMS patients with shorter disease duration (mean of 6.3 years). Interestingly, we observed a trend to increased WM areas in RMS patients compared to controls at C2/C3, but not at any other levels. The observed opposing volumetric effects of WM and GM might be linked to different pathological processes, such as edema/inflammation leading to WM expansion (potentially obfuscating the degree of axonal loss in WM) and neurodegenerative processes leading to cord volume/TCA reduction. Our data suggest that the TCA reduction might be driven primarily by a reduction in GM.

Our results are further corroborated by two recent studies that described microstructural changes in cord GM *in vivo* based on diffusion weighted imaging techniques. These studies demonstrated a high association with MS disability, particularly in progressive MS.[39,40]

Loss of SC neurons, loss of myelin, and additional changes in the neuropil may contribute to SC GM atrophy in MS. Histopathological data demonstrate that there is a 30.3% reduction in total neuronal numbers in the thoracic cord, with significant reductions in motoneurons in myelinated GM.[16] It is not known whether this neuronal loss is directly related to WM damage (e.g. due to anterograde trans-synaptic degeneration, as described for the visual system[41, 42]), whether it reflects an independent neurodegenerative process (caused or worsened by mitochondrial injury), or if it is, at least in part, independent of focal WM damage.[43]

SC GM demyelination can be extensive and exceeds the proportion of demyelinated WM.[44] In contrast to the subpial demyelinating lesions frequently observed in brain tissues in PMS, SC GM demyelination and neuronal loss occur distant from the meninges.[44,45] Changes to the neuropil, such as reductions in synaptic densities, have been described in brain GM[46] but have not been quantified in the SC in MS.

There are a few limitations of this study: We only investigated 4 levels of the cord, not the entire cord. We selected these levels based on anatomic and pathological considerations, and also because a robust segmentation of GM is possible at these levels with a high inter-rater reliability (ICCs of 0.888-0.916, as shown previously).[27] Since a fully automated method is not yet available, GM segmentation was performed manually. Images at the T8/T9 level were more prone to artifacts than the other levels, as indicated by a higher percentage of images (15%) in which segmentation was not possible. This was typically due to motion artifacts. Given the relative high correlations between TCA, cord GM and WM areas of adjacent disc levels, and the results of the analysis of relative importance and partial regression analysis, it seems reasonable to focus future studies on the levels C2/C3 and T9/T10. These levels yield reliable measurements and additive information when used to model EDSS. With regard to the identification of a progressive phenotype, SC GM assessments at each level (in particular at C2/C3, C3/C4, and T9/T10) are clinically informative, though most of the information is already captured by the cervical levels.

The presence of lesions has the potential to confound measurements in a few cases, namely in those in which lesions were located adjacent to the GM, or those in which lesions involved both the GM and WM. In most of these cases, however, one could see a GM/WM

contrast despite the lesion. In those cases where the GM/WM boundary was not visible, the GM boundary was drawn as the shortest line between the two most adjacent clearly distinguishable GM/WM points, respecting the symmetry of the GM structure. Our high level of inter-observer agreement demonstrates that this demarcation is robust. It is possible that lesions in these cases could have impacted either GM or WM area, but the direction of this potential source of bias is difficult to estimate.

Finally, this is a cross-sectional study, thus causal connections cannot be inferred from the results. Future longitudinal studies will be needed to elucidate SC GM changes over time, and their relationship with disability evolution to determine whether SC GM assessments are suited as a biomarker for MS progression.

In conclusion, this study provides evidence for the clinical impact of cord GM atrophy in MS, as measured *in vivo* by PSIR imaging. Cord GM atrophy is present at multiple levels, thus may reflect widespread cord GM degeneration. These results add support to the growing understanding that GM loss is a key mediator of MS disability. The robust relationships between cord GM atrophy and disability are far stronger than those for any known cortical GM or WM metric. Thus, these data, perhaps, suggest a reorientation of current imaging practices. MRI-based estimations of cord GM that have strong correlations with MS disability, may better track the disease process in the context of both clinical trials and longitudinal observational studies.

The central outstanding questions to be answered are 1) what is the temporal relationship of cord GM changes that we observed to the accumulation of MS disability and 2) whether these changes are dependent or independent of focal WM plaques. Longitudinal, prospective studies should help to clarify the role of cord GM changes in monitoring and predicting MS progression.

Supplementary Material

Refer to Web version on PubMed Central for supplementary material.

Acknowledgments

The authors acknowledge Refujia Gomez, Caroline Ciocca, Rachel Kanner, Alan Evangelista, and Adam Santaniello for collection and management of the data.

RS and RH had full access to all of the data in the study and take responsibility for the integrity of the data and the accuracy of the data analysis.

Funding

The authors acknowledge support from research grant funding from the National Multiple Sclerosis Society, The Conrad H. Hilton Foundation, Department of Defense, NIH R01 NS 026799, NIH R01 NS049477, NIH K02 NS072288, National Defense Science and Engineering Fellowship (NDSEG), and Nancy Davis Foundation.

RS has received grants from the Swiss MS Society and the Gottfried and Julia Bangerter-Rhyner Foundation Switzerland.

RH has received grants from Stem Cells Inc, and Roche, outside the submitted work.

JMG is funded by NIH KL2TR000143. He has received compensation for medical legal consulting. AG reports personal fees from Inception Sciences and Mylan Pharmaceuticals and grants/awards from the National Multiple Sclerosis Society, Novartis, UCSF CTSI, and That Man May See as well as philanthropic support from the Rachelff Family and the Robert Dale Family. He also reported serving on an end point adjudication committees for Biogen and Medimmune. He serves on trial steering committees for Novartis and Scientific Advisory Board for Bionure. BC has received personal compensation for consulting from Abbvie, Biogen Idec, EMD Serono, MedImmune, Novartis, Genzyme/sanofi aventis, Teva Neurosciences and has received contracted research support (including clinical trials) from Acorda, Avanir, Biogen Idec, EMD Serono, Hoffman La Roche, MedImmune and Teva Neurosciences.

SLH currently serves on the SAB of Symbiotix, Annexon, and Bionure.

Role of the Funder/Sponsor: The funding sources had no role in the design and conduct of the study; collection, management, analysis, and interpretation of the data; preparation, review, or approval of the manuscript; and decision to submit the manuscript for publication.

References

1. Kidd D, Thorpe JW, Thompson AJ, Kendall BE, Moseley IF, MacManus DG, et al. Spinal cord MRI using multi-array coils and fast spin echo. II Findings in multiple sclerosis. Neurology. 1993; 43:2632–2637. [PubMed: 8255468]
2. Lin X, Tench CR, Evangelou N, Jaspan T, Constantinescu CS. Measurement of spinal cord atrophy in multiple sclerosis. J Neuroimaging. 2004; 14:20–26.
3. Bakshi R, Dandamudi VS, Neema M, De C, Bermel RA. Measurement of brain and spinal cord atrophy by magnetic resonance imaging as a tool to monitor multiple sclerosis. J Neuroimaging. 2005; 15:30–45.
4. Lin X, Tench CR, Turner B, Blumhardt LD, Constantinescu CS. Spinal cord atrophy and disability in multiple sclerosis over four years: application of a reproducible automated technique in monitoring disease progression in a cohort of the interferon beta-1a (Rebif) treatment trial. J Neurol Neurosurg Psychiatry. 2003; 74:1090–1094. [PubMed: 12876240]
5. Kalkers NF, Barkhof F, Bergers E, van Schijndel R, Polman CH. The effect of the neuroprotective agent riluzole on MRI parameters in primary progressive multiple sclerosis: a pilot study. Mult Scler. 2002; 8:532–533. [PubMed: 12474997]
6. Leary SM, Miller DH, Stevenson VL, Brex PA, Chard DT, Thompson AJ. Interferon beta-1a in primary progressive MS: an exploratory, randomized, controlled trial. Neurology. 2003; 60:44–51. [PubMed: 12525716]
7. Montalban X, Sastre-Garriga J, Tintoré M, Brieva L, Aymerich FX, Río J, et al. A single-center, randomized, double-blind, placebo-controlled study of interferon beta-1b on primary progressive and transitional multiple sclerosis. Mult Scler. 2009; 15:1195–1205. [PubMed: 19797261]
8. Losseff NA, Webb SL, O'Riordan JI, Page R, Wang L, Barker GJ, et al. Spinal cord atrophy and disability in multiple sclerosis A new reproducible and sensitive MRI method with potential to monitor disease progression. Brain. 1996; 119:701–708. [PubMed: 8673483]
9. Bieniek M, Altmann DR, Davies GR, Ingle GT, Rashid W, Sastre-Garriga J, et al. Cord atrophy separates early primary progressive and relapsing remitting multiple sclerosis. J Neurol Neurosurg Psychiatry. 2006; 77:1036–1039. [PubMed: 16793860]
10. Rocca MA, Horsfield MA, Sala S, Copetti M, Valsasina P, Mesaros S, et al. A multicenter assessment of cervical cord atrophy among MS clinical phenotypes. Neurology. 2011; 76:2096–2102. [PubMed: 21670439]
11. Bonati U, Fisniku LK, Altmann DR, Yiannakas MC, Furby J, Thompson AJ, et al. Cervical cord and brain grey matter atrophy independently associate with long-term MS disability. J Neurol Neurosurg Psychiatry. 2011; 82:471–472. [PubMed: 20710012]
12. Kearney H, Rocca MA, Valsasina P, Balk L, Sastre-Garriga J, Reinhardt J, et al. Magnetic resonance imaging correlates of physical disability in relapse onset multiple sclerosis of long disease duration. Mult Scler. 2014; 20:72–80. [PubMed: 23812283]
13. Ganter P, Prince C, Esiri MM. Spinal cord axonal loss in multiple sclerosis: a post-mortem study. Neuropathol Appl Neurobiol. 1999; 25:459–467. [PubMed: 10632896]

14. Bjartmar C, Kidd G, Mörk S, Rudick R, Trapp BD. Neurological disability correlates with spinal cord axonal loss and reduced N-acetyl aspartate in chronic multiple sclerosis patients. Ann Neurol. 2000; 48:893–901. [PubMed: 11117546]
15. DeLuca GC, Ebers GC, Esiri MM. Axonal loss in multiple sclerosis: a pathological survey of the corticospinal and sensory tracts. Brain. 2004; 127:1009–1018. [PubMed: 15047586]
16. Gilmore CP, DeLuca GC, Bö L, Owens T, Lowe J, Esiri MM, et al. Spinal cord neuronal pathology in multiple sclerosis. Brain Pathol. 2009; 19:642–649. [PubMed: 19170682]
17. Bot JC, Blezer EL, Kamphorst W, Lycklama A, Nijeholt GJ, Ader HJ, et al. The spinal cord in multiple sclerosis: relationship of high-spatial-resolution quantitative MR imaging findings to histopathologic results. Radiology. 2004; 233:531–540. [PubMed: 15385682]
18. Gilmore CP, DeLuca GC, Bö L, Owens T, Lowe J, Esiri MM, et al. Spinal cord atrophy in multiple sclerosis caused by white matter volume loss. Arch Neurol. 2005; 62:1859–1862. [PubMed: 16344343]
19. Grinberg LT, Amaro E Jr, Teipel S, dos Santos DD, Pasqualucci CA, Leite RE, et al. Brazilian Aging Brain Study Group. Assessment of factors that confound MRI and neuropathological correlation of human postmortem brain tissue. Cell Tissue Bank. 2008; 9:195–203. [PubMed: 18548334]
20. Kretschmann HJ, Tafesse U, Herrmann A. Different volume changes of cerebral cortex and white matter during histological preparation. Microsc Acta. 1982; 86:13–24. [PubMed: 7048029]
21. Dietrich O, Reiser MF, Schoenberg SO. Artifacts in 3-T MRI: physical background and reduction strategies. European Journal of Radiology. 2008; 65:29–35. [PubMed: 18162353]
22. Stroman PW, Wheeler-Kingshott C, Bacon M, Schwab JM, Bosma R, Brooks J, et al. The current state-of-the-art of spinal cord imaging: methods. Neuroimage. 2014; 84:1070–1081. [PubMed: 23685159]
23. Kellman P, Arai AE, McVeigh ER, Aletras AH. Phase-sensitive inversion recovery for detecting myocardial infarction using gadolinium-delayed hyperenhancement. Magn Reson Med. 2002; 47:372–383. [PubMed: 11810682]
24. Huber AM, Schoenberg SO, Hayes C, Spannagl B, Engelmann MG, Franz WM, et al. Phase-sensitive inversion-recovery MR imaging in the detection of myocardial infarction. Radiology. 2005; 237:854–860. [PubMed: 16304107]
25. Kearney H, Miszkiel KA, Yiannakas MC, Ciccarelli O, Miller DH. A pilot study of white and grey matter involvement by multiple sclerosis spinal cord lesions. Multiple Sclerosis and Related Disorders. 2013; 2:103–108. [PubMed: 25877631]
26. Kearney H, Yiannakas MC, Abdel-Aziz K, Wheeler-Kingshott CA, Altmann DR, Ciccarelli O, et al. Improved MRI quantification of spinal cord atrophy in multiple sclerosis. J Magn Reson Imaging. 2014; 39:617–623. [PubMed: 23633384]
27. Papinutto N, Schlaeger R, Panara V, Caverzasi E, Ahn S, Johnson KJ, et al. 2D phase-sensitive inversion recovery imaging to measure in vivo spinal cord gray and white matter areas in clinically feasible acquisition times. J Magn Reson Imaging. 2014; doi: 10.1002/jmri.24819
28. Schlaeger R, Papinutto N, Panara V, Bevan C, Lobach IV, Bucci M, et al. Spinal cord gray matter atrophy correlates with multiple sclerosis disability. Ann Neurol. 2014; 76:568–580. [PubMed: 25087920]
29. Polman CH, Reingold SC, Banwell B, Clanet M, Cohen JA, Filippi M, et al. Diagnostic criteria for multiple sclerosis: 2010 revisions to the McDonald criteria. Ann Neurol. 2011; 69:292–302. [PubMed: 21387374]
30. Kurtzke JF. Rating neurologic impairment in multiple sclerosis: an expanded disability status scale (EDSS). Neurology. 1983; 33:1444–1452. [PubMed: 6685237]
31. Kappos, L., Lechner-Scott, J., Wu, S. Neurostatus.net: Independent internet platform for training and certification of physicians participating in projects that use a standardised, quantified neurological examination and assessment of Kurtzke's Functional Systems and Expanded Disability Status Scale in Multiple Sclerosis. 2009. Version 9/2008http://www.neurostatus.net
32. Fischer JS, Rudick RA, Cutter GR, Reingold SC. The Multiple Sclerosis Functional Composite Measure (MSFC): an integrated approach to MS clinical outcome assessment National MS Society Clinical Outcomes Assessment Task Force. Mult Scler. 1999; 5:244–250. [PubMed: 10467383]

33. Horsfield MA, Sala S, Neema M, Absinta M, Bakshi A, Sormani MP, et al. Rapid semi-automatic segmentation of the spinal cord from magnetic resonance images: application in multiple sclerosis. Neuroimage. 2010; 50:446–455. [PubMed: 20060481]
34. Groemping U. Relative Importance for Linear Regression in R: The Package relaimpo. Journal of Statistical Software. 2006; 17
35. Genizi A. Decomposition of R2 in multiple regression with correlated regressors. Statistica Sinica. 1993; 3:407–420.
36. Lublin FD, Reingold SC, Cohen JA, Cutter GR, Sørensen PS, Thompson AJ, et al. Defining the clinical course of multiple sclerosis: the 2013 revisions. Neurology. 2014; 83:278–286. [PubMed: 24871874]
37. Liu W, Nair G, Vuolo L, Bakshi A, Massoud R, Reich DS, et al. In vivo imaging of spinal cord atrophy in neuroinflammatory diseases. Ann Neurol. 2014; 76:370–378. [PubMed: 25042583]
38. Klein JP, Arora A, Neema M, Healy BC, Tauhid S, Goldberg-Zimring D, et al. A 3T MR imaging investigation of the topography of whole spinal cord atrophy in multiple sclerosis. AJNR Am J Neuroradiol. 2011; 32:1138–1142. [PubMed: 21527570]
39. Raz E, Bester M, Sigmund EE, Tabesh A, Babb JS, Jaggi H, et al. A better characterization of spinal cord damage in multiple sclerosis: a diffusional kurtosis imaging study. AJNR Am J Neuroradiol. 2013; 34:1846–1852. [PubMed: 23578677]
40. Kearney H, Schneider T, Yiannakas MC, Altmann DR, Wheeler-Kingshott CA, Ciccarelli O, et al. Spinal cord grey matter abnormalities are associated with secondary progression and physical disability in multiple sclerosis. J Neurol Neurosurg Psychiatry. Aug 5.2014 doi: 10.1136/jnnp-2014-308241
41. Gabilondo I, Martínez-Lapiscina EH, Martínez-Heras E, Fraga-Pumar E, Llufriu S, Ortiz S, et al. Trans-synaptic axonal degeneration in the visual pathway in multiple sclerosis. Ann Neurol. 2014; 75(1):98–107. [PubMed: 24114885]
42. Balk LJ, Steenwijk MD, Tewarie P, Daams M, Killestein J, Wattjes MP, et al. Bidirectional trans-synaptic axonal degeneration in the visual pathway in multiple sclerosis. J Neurol Neurosurg Psychiatry. 2015; 86(4):419–424. [PubMed: 24973342]
43. Calabrese M, Magliozzi R, Ciccarelli O, Geurts JJ, Reynolds R, Martin R. Exploring the origins of grey matter damage in multiple sclerosis. Nat Rev Neurosci. 2015; 16:147–158. [PubMed: 25697158]
44. Gilmore CP, Bö L, Owens T, Lowe J, Esiri MM, Evangelou N. Spinal cord gray matter demyelination in multiple sclerosis-a novel pattern of residual plaque morphology. Brain Pathol. 2006; 16:202–208. [PubMed: 16911477]
45. Magliozzi R, Howell OW, Reeves C, Roncaroli F, Nicholas R, Serafini B, et al. A Gradient of neuronal loss and meningeal inflammation in multiple sclerosis. Ann Neurol. 2010; 68:477–493. [PubMed: 20976767]
46. Wegner C, Esiri MM, Chance SA, Palace J, Matthews PM. Neocortical neuronal, synaptic, and glial loss in multiple sclerosis. Neurology. 2006; 67:960–967. [PubMed: 17000961]

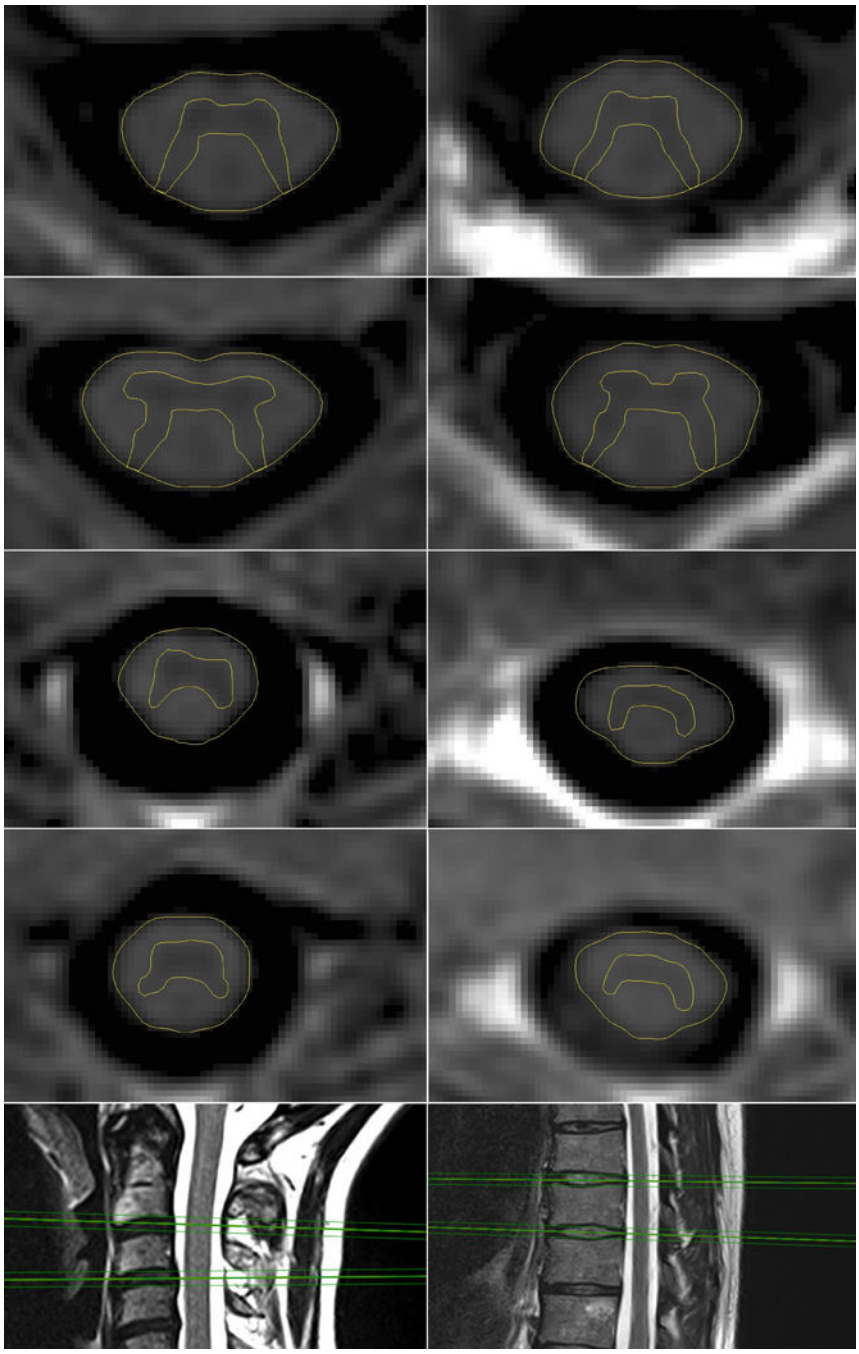

Figure 1. A-J. Phase sensitive inversion recovery images illustrating gray matter atrophy in Multiple Sclerosis

Axial 2D-phase sensitive inversion (PSIR) images at the intervertebral disc levels C2/C3, C3/C4, T8/T9 and T9/T10 of a woman with RMS and EDSS 1.0 (A, B, C, D) and an age-matched woman with primary progressive MS, EDSS 4.0 (E, F, G, H, respectively) illustrating GM atrophy in progressive MS. Segmentation of the cord area was conducted semi-automatically using an active surface model. Segmentation of the gray matter area was performed manually. Acquisition of the images perpendicular to the cord at the intervertebral disc levels C2/C3, C3/C4 (I), T8/T9 and T9/T10 (J).

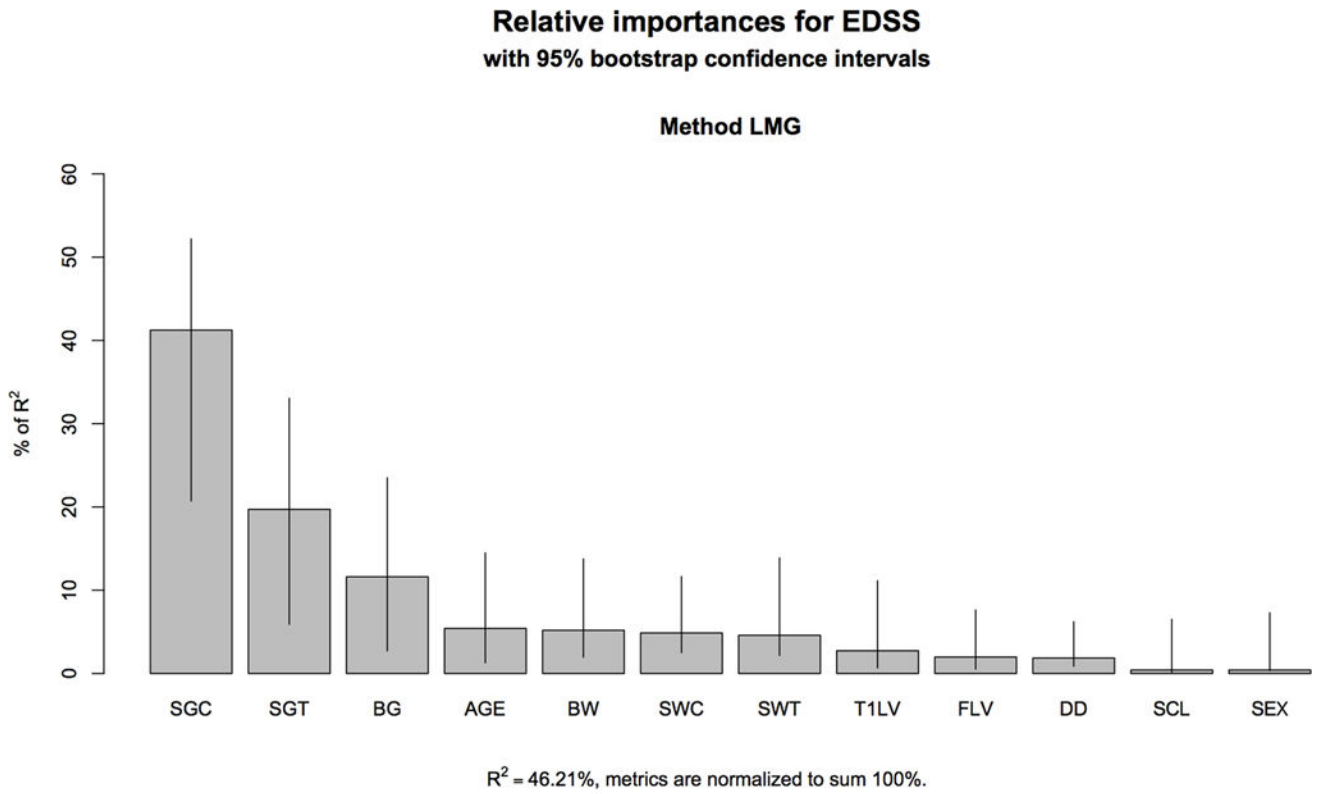

Figure 2. Relative contributions of demographic, clinical and imaging variables to the Expanded Disability Status Scale

Relative contributions of the variables (cervical spinal cord gray matter (SGC) and white matter (SWC) areas at C2/C3, thoracic spinal cord gray matter (SGT) and white matter (SWT) at T9/T10, normalized brain gray matter volume (BG) and normalized brain white matter volume (BW), the number of spinal cord T2 lesions (SCL), brain T1 lesion volume (T1LV), brain FLAIR lesion volume (FLV), age, sex, and disease duration (DD)) to the Expanded Disability Status Score (EDSS) using a linear model.

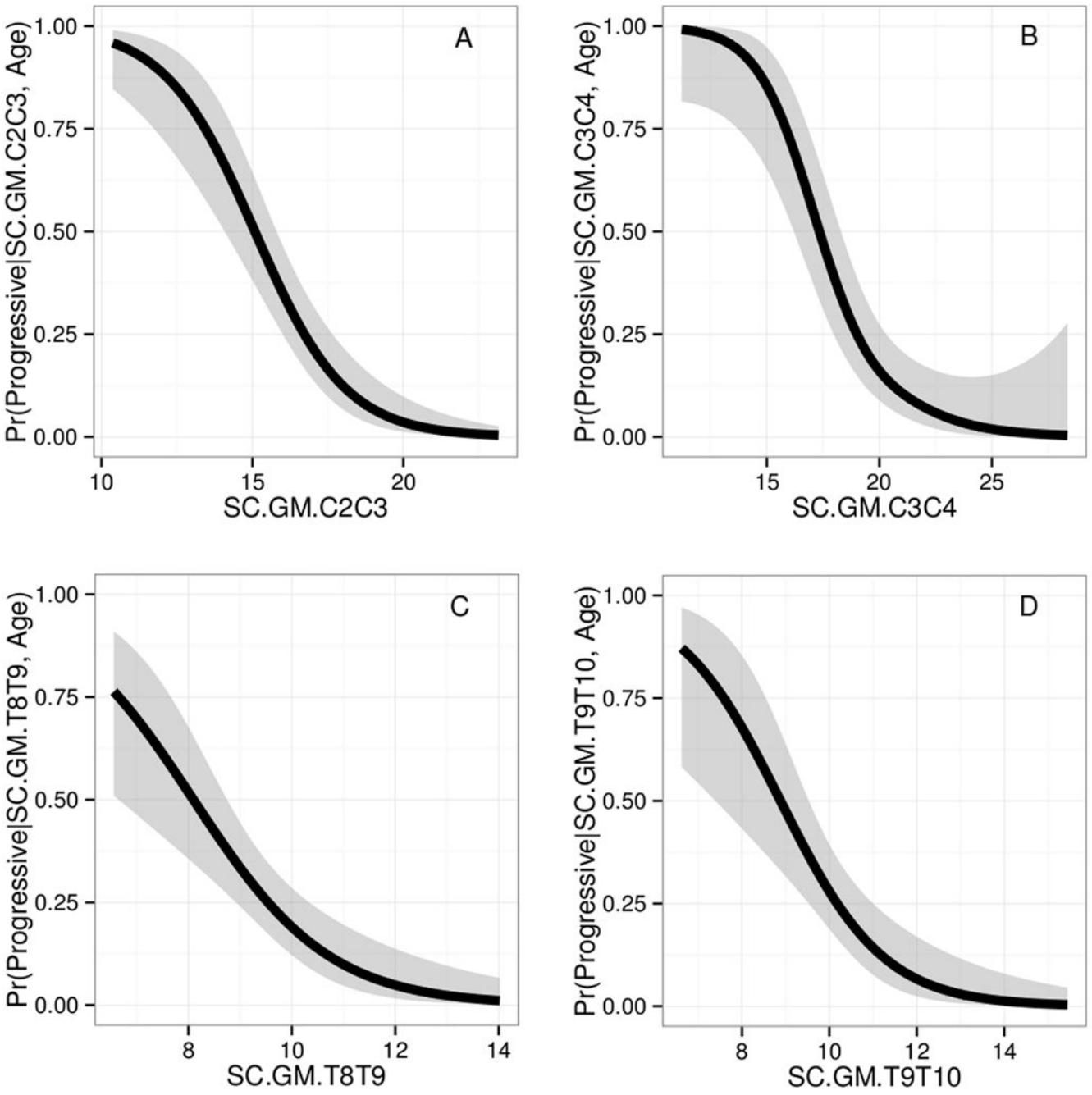

Figure 3. A-D. Probability maps of a progressive disease course based on spinal cord gray matter assessments

Probability of a progressive disease course adjusted for age as assessed by spinal cord GM area (x-axis, in mm^2) at the levels C2/C3 (A), C3/C4 (B), T8/T9 (C), and T9/T10 (D). Gray shades indicate 95% confidence intervals.

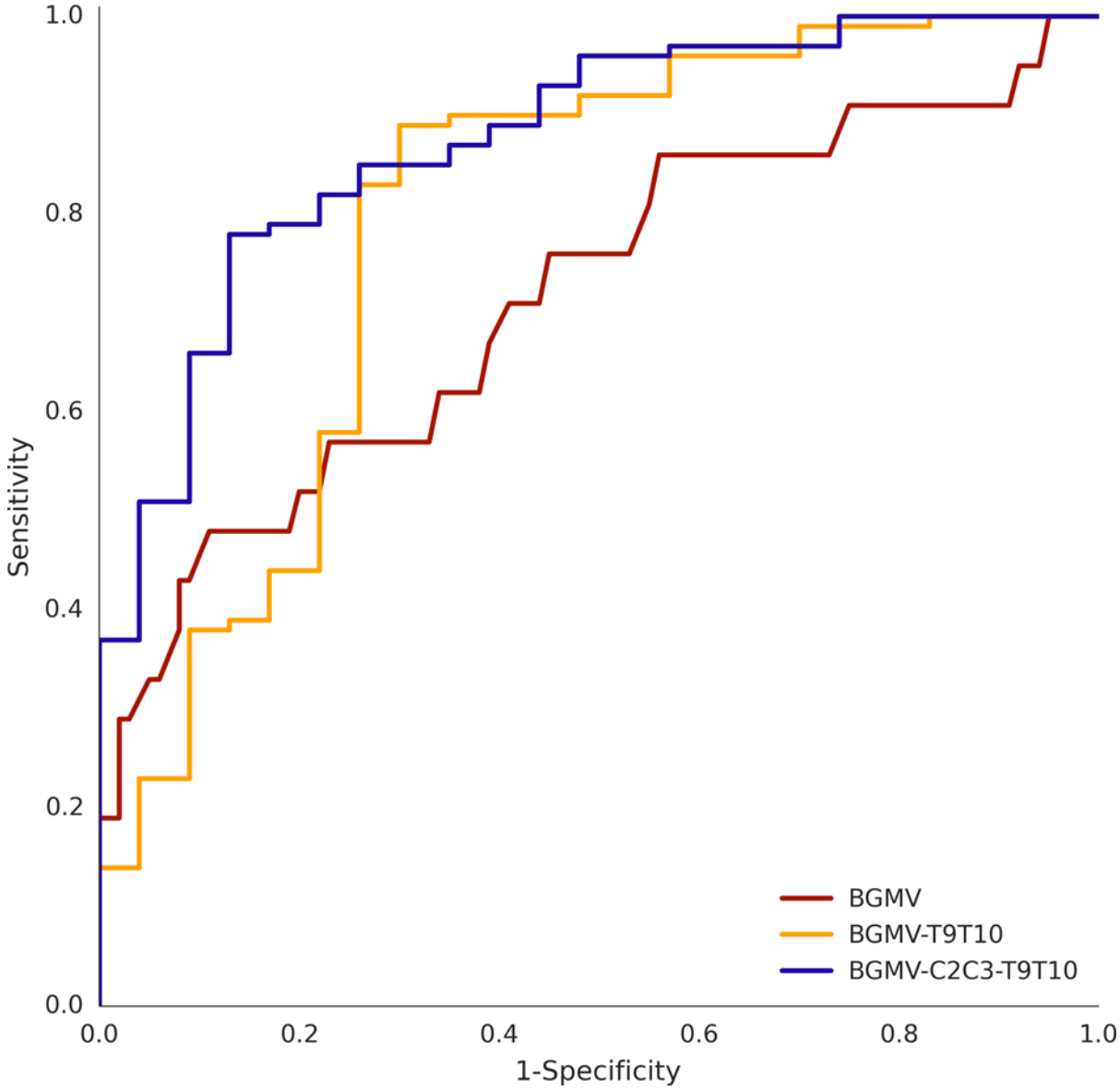

Figure 4. Receiver operating characteristic curves for the prediction of a progressive disease course based on gray matter assessments

Receiver operating characteristic (ROC) curves for the prediction of a progressive versus relapsing disease course by binary logistic models with a) the normalized brain gray matter (GM) volume as single predictor (red line), b) the normalized brain GM volume along with the thoracic spinal cord GM area at T9/T10 (yellow line) and c) the normalized brain GM volume along with the spinal cord GM areas at C2/C3 and T9/T10 (violet line) as combined predictors. The areas under the curve (AUC) were 0.68, 0.79 and 0.87, respectively.

Table 1

Comparison of cervical PSIR imaging derived measures between controls, patients with relapsing (RMS) and progressive disease courses (PMS) using linear regression with age and sex as covariates

Disc level	PSIR measure	Group	Adj. mean	StdErr (mean)	Mean diff.	StdErr (diff.)	P	95%-Confidence Interval (diff.)	
C2/C3	Mean GM area (mm^2)	Controls RMS PMS	20.53 18.20 15.00	0.47 0.23 0.37	2.34 3.20	0.52 0.44	**<0.0001** **<0.0001**	1.31 2.32	3.37 4.07
	Mean WM area (mm^2)	Controls RMS PMS	57.66 59.33 55.42	1.57 0.75 1.21	-1.67 3.91	1.71 1.46	0.3323 **0.0082**	-5.06 1.03	1.72 6.79
	TCA (mm^2)	Controls RMS PMS	78.44 77.46 68.12	2.02 0.94 1.43	0.98 9.34	2.20 1.75	0.6563 **<0.0001**	-3.37 5.90	5.33 12.79
C3/C4	Mean GM area (mm^2)	Controls RMS PMS	22.07 21.19 17.29	0.56 0.28 0.46	0.89 3.90	0.62 0.56	0.1550 **<0.0001**	-0.34 2.80	2.11 5.00
	Mean WM area (mm^2)	Controls RMS PMS	59.92 59.68 55.21	1.72 0.87 1.43	0.25 4.46	1.90 1.71	0.8974 **0.0103**	-3.53 1.07	4.02 7.85
	TCA (mm^2)	Controls RMS PMS	82.31 80.37 71.46	2.16 1.07 1.65	1.94 8.91	2.38 2.01	0.4168 **<0.0001**	-2.77 4.93	6.66 12.88
T8/T9	Mean GM area (mm^2)	Controls RMS PMS	11.17 10.19 9.16	0.30 0.14 0.25	0.98 1.02	0.32 0.29	**0.0030** **0.0006**	0.34 0.45	1.62 1.60
	Mean WM area (mm^2)	Controls RMS PMS	33.29 32.05 30.58	0.94 0.44 0.78	1.23 1.47	1.03 0.93	0.2316 0.1156	-0.80 -0.37	3.28 3.30
	TCA (mm^2)	Controls RMS PMS	44.49 42.40 38.74	1.18 0.52 0.82	2.09 3.66	1.28 0.99	0.1047 **0.0003**	-0.44 1.69	4.63 5.62
T9/10	Mean GM area (mm^2)	Controls RMS PMS	12.04 11.11 9.73	0.33 0.16 0.30	0.93 1.37	0.36 0.35	**0.0110** **<0.0001**	0.22 0.69	1.65 2.06
	Mean WM area (mm^2)	Controls RMS PMS	33.42 32.81 31.55	0.91 0.46 0.83	0.61 1.26	1.00 0.96	0.5478 0.1917	-1.38 -0.64	2.59 3.17
	TCA (mm^2)	Controls RMS PMS	45.50 43.90 40.87	1.12 0.55 0.86	1.60 3.04	1.23 1.04	0.1983 **0.0042**	-0.84 0.97	4.02 5.10

Mean values are least square means with adjustment for age and sex. Mean differences: first line refers to the difference between controls and RMS; second line refers to the difference between RMS and PMS. Adj.: adjusted; StdErr: standard error, Diff.: difference between means, TCA: total cord area, GM: gray matter, WM: white matter area. P-values are 2-sided.